Finite Element Analysis Method for Detection of the Corona Discharge Inception Voltage in a Wire-Cylinder Arrangement

Conference Paper · May 2013

CITATIONS
4

READS
859

3 authors:

Konstantinos Kiousis
University of West Attica
16 PUBLICATIONS **106** CITATIONS
SEE PROFILE

Antonios Moronis
University of West Attica
40 PUBLICATIONS **358** CITATIONS
SEE PROFILE

Emmanouil D. Fylladitakis
University of West Attica
40 PUBLICATIONS **559** CITATIONS
SEE PROFILE

Finite Element Analysis Method for Detection of the Corona Discharge Inception Voltage in a Wire-Cylinder Arrangement

KONSTANTINOS N. KIOUSIS, ANTONIOS X. MORONIS, EMMANOUIL D. FYLLADITAKIS
Technological Educational Institute (TEI) of Athens
Energy Technology Department
Ag. Spyridonos 12210 Aegaleo
GREECE
konstantinosq@gmail.com, amoronis@teiath.gr, et.e.f.gr@gmail.com

Abstract: The inception voltage of the positive corona discharges (*CIV*) in a typical *wire-cylinder* electrode arrangement in air, under high voltage dc application, has been studied by implementing the *Finite Element Analysis (FEA)*. Numerical analysis has been carried out on the electric field intensity, along the wire-cylinder gap axis, in order to determine the inception voltage of each air gap and define its dependence on geometrical characteristics of the electrodes. An experimental investigation has been conducted and used so as to justify the simulation results. The *CIV* was mainly associated to the wire radius, while the distance between the electrodes had a secondary importance. Finally, the inception voltage had slight changes for different cylinder radii.

Key-Words: Finite Element Analysis (*FEA*), Corona Inception Voltage (*CIV*), Wire-cylinder arrangement

1 Introduction

In recent years, the corona discharge phenomenon has been the subject of intensive studies [1-3]. Corona discharges have been a main concern for power transmission engineers because of the associated power loss, audible noise and signal interference [4]. On the other hand the sustainable corona discharge process is widely used as the source of unipolar ions in a number of commercial and industrial applications [5-8] and generally applications where small particle or droplet motion control is needed [9-11]. In any case, the main criterion is the threshold voltage in which the corona discharges initiate (*Corona Inception Voltage*) [12].

The corona inception voltage (*CIV*) has been investigated by Peek who thereby developed some well-known empirical formulae [13]. Successful attempts have been made since then, in order to relate the inception of the corona discharges with geometry and environmental parameters [14-17], but there is no study available for the parallel *wire-cylinder* arrangement. On the other hand, investigations by means of the electric field and potential distribution as well as the corona discharge current measurements, have already been conducted for *wire-cylinder* electrode pairs [18-20].

The goal of this paper is the fine modeling and analysis of the electric field strength in a *wire-cylinder* configuration in air, in order to define the threshold voltage of the corona discharges, considering the geometrical characteristics of the electrodes.

2 Corona Inception Voltage (*CIV*)

Corona discharge is a process where current develops from an electrode, by ionizing the surrounding medium near sharp points or edges. The ionization region for parallel conductors can be calculated as [13]:

$$a = 0.301 \cdot \sqrt{r} \qquad (1)$$

where r [cm] is the radius of the emitter (wire).

Once the field intensity is sufficient, the degree of field non-uniformity is high enough and free electrons are available in the overstressed field region a, corona discharges initiate. The threshold voltage *(CIV*) between two parallel conductors is given by Peek's formula [13]:

$$CIV = m_u \cdot g_o \cdot \left(1 + 0.301 \Big/ \sqrt{\delta \cdot r}\right) \cdot r \cdot \ln\left(\frac{d}{r}\right) \qquad (2)$$

where m_u represents the emitter's roughness factor (m_u=1 for smooth polished wires), g_o is the air's dielectric strength ($\sim 3 \cdot 10^6 V/m$), d [m] is the electrode gap and δ is the air density factor (*for STP conditions, δ=1*). As soon as the corona discharges initiate in the vicinity of the overstressed electrode (*wire*), space charge accumulates, which in turn produces current flow (*corona discharge current*) as ionized air molecules drift (*corona gap*) towards the collector (*cylinder*).

Several numerical and experimental methods have been proposed for the determination of the *CIV* [21]. In the present study, simulation results will be compared with experimental findings in order to ensure the accuracy of the applied method.

ISBN: 978-1-61804-184-5

3 Electrode geometry and dimensions

The electrode pair and its critical dimensions (wire radius *r*, cylinder radius *R* and electrode gap *d*), are shown in Fig. 1. Since the corona inception voltage is strongly dependent on the electric field non-uniformity, different *R/r* and *d/r* ratios have been used as shown in table 1.

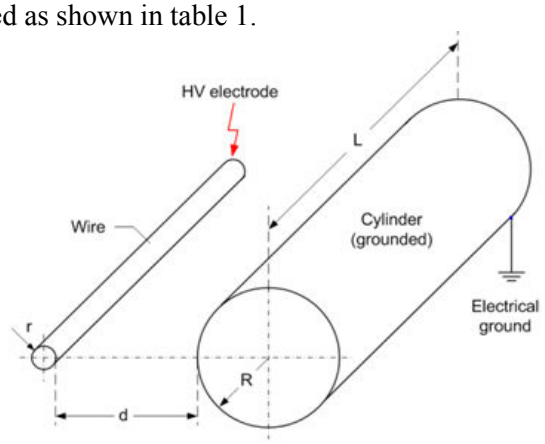

Fig. 1 The *wire-cylinder* electrode pair

Table 1 Geometrical characteristics and dimensions

Geometrical characteristic	*Dimensions*
Gap distance d (cm)	*1,2,3,4,5*
Wire radius r (μm)	*30,50,100,250,400*
Cylinder radius R (mm)	*5,10,15,20*
R/r ratio	*12.5 - 667*
d/r ratio	*75 - 1667*

4 Numerical Model and Parameters

A dedicated simulation software *FEMM (ver.4.2)*, implementing the *Finite Element Analysis,* has been used for the present study. In our case, the steady state electrostatics problem is governed by the well-known Gauss's and Poisson's equations:

$$E = -\nabla V \tag{3}$$

$$\nabla^2 V = -\rho / \varepsilon_0 \tag{4}$$

where E $[V/m]$ is the electric field, V $[V]$ is the applied voltage, ρ $[C/m^3]$ is the space charge density in the region, and ε_0 represents the dielectric permittivity of free space ($\sim 8.85 \cdot 10^{-12}$ *F/m* in air).

The electric field should satisfy the charge conservation law:

$$\nabla \cdot j = 0 \tag{5}$$

where j $[A/m^2]$ is the current density, defined as:

$$j = \rho \cdot \mu \cdot E \tag{6}$$

where μ $[m^2/V \cdot s]$ is the dielectric's ion mobility.

Equations (3-6) can be combined to obtain:

$$\nabla \cdot \left\{ \left(\nabla^2 V \right) \left(\nabla V \right) \right\} = 0 \tag{7}$$

FEMM solves (7), for potential V, over a user defined domain with user defined sources and boundary conditions. Due to the longitudinal axis symmetry, the electric field distribution may only change in the radial direction, along the electrode gap thus, a 3-dimensional problem may be minimized into a 2-dimensional problem that requires a much smaller number of nodes and less computing power. Hence, a 2-dimensional planar electrostatic problem has been defined, with a solver precision value of 10^{-8}.

Because of the symmetry of the *wire-cylinder* geometry along the gap axis, half-plane modeling has been applied and the problem's domain was defined by a proper bounding box, so as to certify accuracy and, at the same time, keep low the demand for computing power and time [19].

The key parameters to the *FEMM* model such as the *maximum arc segment angle*, *minimum angle of the triangular mesh*, *local element size along line* and *mesh size*, have been analytically studied so as to ensure appropriate mesh formation in order to accomplish convergence of the results. In this way an optimal mesh with a dense formation near areas of interest has been configured (see Fig. 2), in terms of accuracy and processing power as well [19].

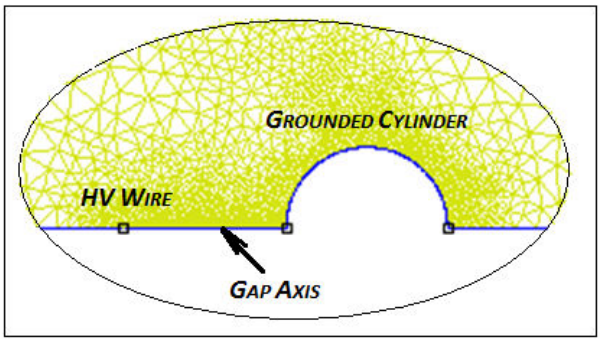

Fig. 2 Optimized mesh formation
(Detailed area of interest near the Wire and the Cylinder)

Dirichlet conditions [22] have explicitly been defined in order to fix the voltage of the wire's surface in the problem's domain. The stressed electrode was the wire, with prescribed voltage $V_{WIRE}=1000V$, while the cylindrical electrode was electrically grounded ($V_{CYLINDER}=0V$).

It should be noted that in this way, the electric field strength at αkV potential equals α times the electric field at *1kV*. Hence, the *CIV* $[kV]$ may be determined in each case by dividing the air's dielectric strength ($\sim 3 \cdot 10^6 V/m$) with the electric field strength at the vicinity of the ionization region *a*.

$$CIV_{SIMULATION} = \left(Air's\ Dielectric\ Strength \right) / E_a \tag{8}$$

5 Experimental Setup

In order to investigate the inception of the corona discharges experimentally, a set of *wire-cylinder* electrode pairs has been carefully prepared. Each module consisted of a thin polished copper wire with radius *r* (*emitter*) and an aluminum cylinder (*collector*) with radius *R*, while the electrode length was *L*. Both electrodes were fixed on a wooden frame parallel to each other, at distance *d* (*corona gap*) and placed in ambient air (*dielectric medium*).

Positive high dc voltage has been applied to the emitter by an adjustable high voltage dc power source (*Matsusada Precision W Series*), while the collector was connected to the electrical ground. The positive corona discharge current was measured by a *Metra Hit 28S* precision multimeter connected in series between the collector and the ground as shown in Fig. 3.

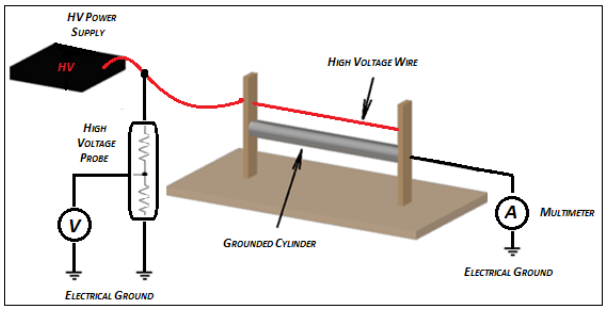

Fig. 3 Experimental setup with the wire-cylinder pair

In order to detect the inception voltage of the positive corona discharges, the voltage step near the discharge region was *50Volts*.

An indicative representation of the *CIV* detection is shown below, in Fig. 4. In this case the electrode length was *500mm*, the electrode gap *3cm* and the wire and cylinder radii were *50μm* and *15mm* respectively.

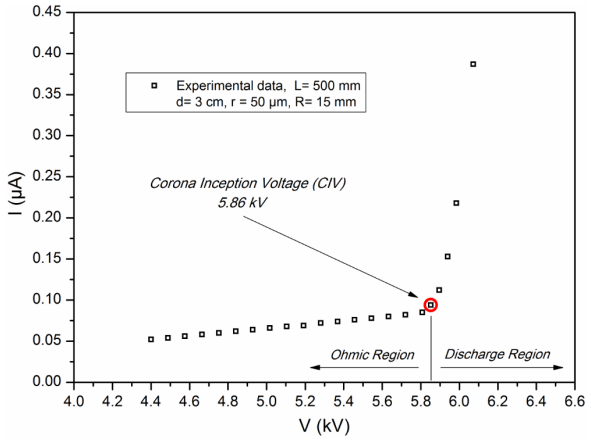

Fig. 4 Corona Inception Voltage detection method
(*L=500mm, d=3cm, r=50μm and R=15mm*)

As shown in Fig. 4, in the region below *5.86kV* (*CIV*), where the electric field is relatively small, the dielectric medium exhibits an Ohmic behaviour (*Ohmic Region*). When the applied voltage is further increased, above the inception voltage (*Corona Discharge Region*), corona discharges initiate and the *V/I* characteristic may then be expressed by Townsend's quadratic relationship [23].

6 Results and Discussion

Analysis of the positive corona inception voltage in air, in the case of a *wire-cylinder* arrangement has been carried out for different electrode radii and gap values (*R/r÷12.5-667* and *d/r ÷ 75-1667*).

Fig.5 shows the electric field distribution in the case of the *wire-cylinder* geometry. The wire radius was *50μm*, the cylinder radius *15mm* and the electrode gap *3cm*. The simulation results have shown that the maximum electric field strength E_{max} is located at the outer surface of the wire electrode, at the least distant point from the cylinder.

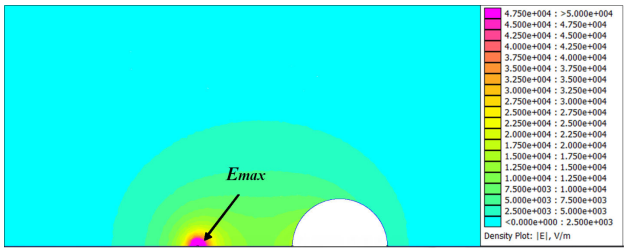

Fig. 5 Electric field distribution in a *wire-cylinder* arrangement
(*d=3cm, r=50μm and R=15mm*, *1kV* potential difference)

On the other hand, Fig. 6 is a detailed plot of the electric field distribution near the hv wire electrode (E_{max}) and the surrounding area of the ionization region *a* (E_a).

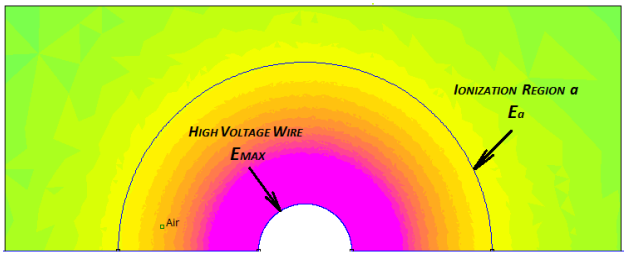

Fig. 6 Electric Field Distribution
Area near the hv wire and the Ionization Region *a*

Comparisons between the *FEMM* simulation results, along with the experimental results and empirical values according to Peek's formula for the corona inception voltage (2) are presented in the figures below.

ISBN: 978-1-61804-184-5

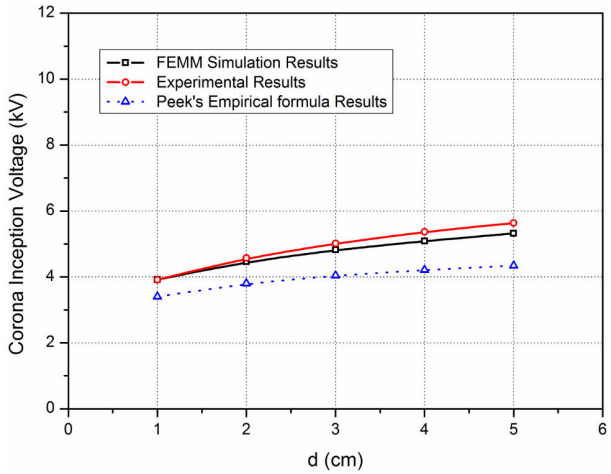

Fig. 7 Dependence of the *CIV* on the electrode gap *d* (*L=500mm, r=50μm and R=15mm*)

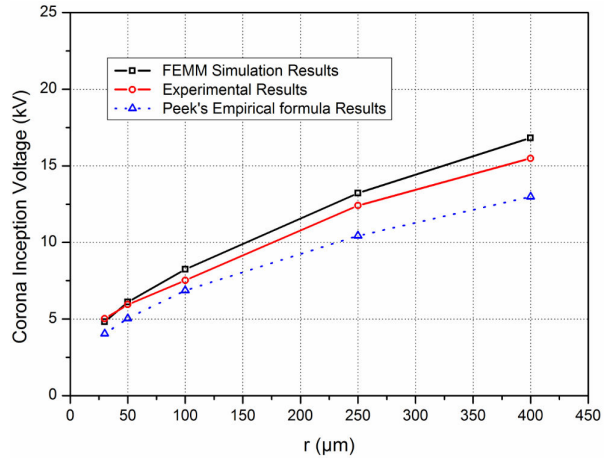

Fig. 8 Dependence of the *CIV* on the wire radius *r* (*L=500mm, d=3cm and R=15mm*)

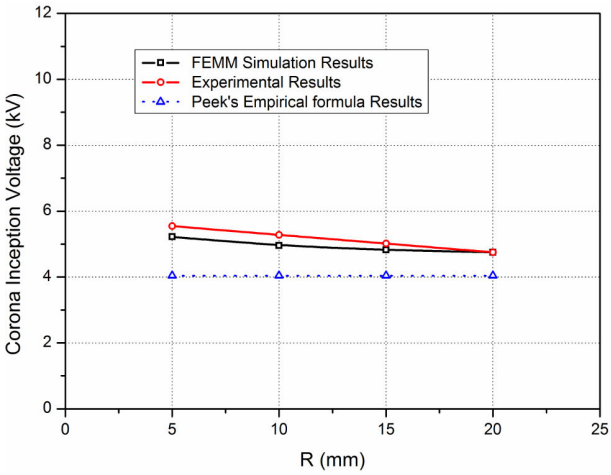

Fig. 9 Dependence of the *CIV* on the cylinder radius *R* (*L=500mm, d=3cm and r=50μm*)

As shown in Fig. 7 and Fig. 8, the inception voltage increases with the electrode gap *d* and the wire radius *r*, while on the other hand, decreases with the cylinder radius *R* (see Fig. 9).

Small gaps and wire radii produce higher electric field magnitude in the conductor's surface, which in turns reduces the inception voltage of the corona discharges. As far as the cylinder radius is concerned, larger cylinders produce higher field inhomogeneities and as a result, reduced inception voltage values.

As shown in the figures above, the experimental results were in a good agreement with simulations data, thus confirming the accuracy of the applied method. On the other hand, Peek's empirical formula results according to (2) had slight divergence which may be attributed to the electric field which is less homogeneous in the *wire-cylinder* arrangement, compared to the parallel wire's geometry (see figure 10).

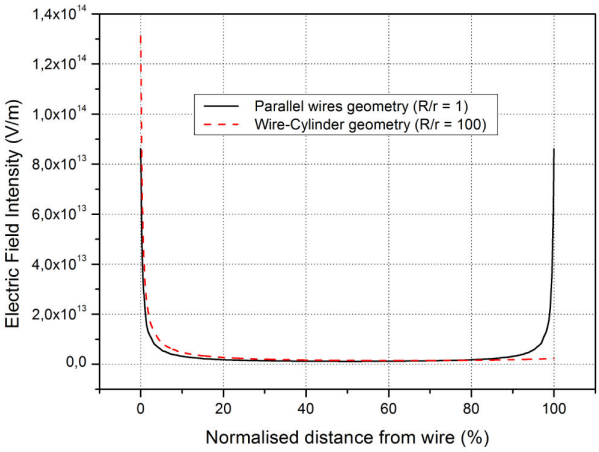

Fig. 10 Electric field intensity along the normalised electrode gap (%), for parallel wire geometry (*R/r=1*) and wire-cylinder geometry (*R/r=100*)

An empirical formula for the estimation of the maximum electric field intensity of the air gap (*at the conductor's surface*) the exact moment when the corona discharges initiate, has also been derived by Peek [13]:

$$E_{CIV} = m_u \cdot g_o \cdot \left(1 + 0.301 \Big/ \sqrt{\delta \cdot r}\right) \qquad (9)$$

In our case, the electric field magnitude that has been determined at the conductor's surface (at *1kV*) multiplied by the corona inception voltage (*CIV*) provides the value of the field intensity at the exact moment when the positive corona discharges initiate.

A correlation between *FEMM* simulation results for the electric field magnitude at the inception voltage and Peek's empirical formula values according to (9) are presented in the following figures.

ISBN: 978-1-61804-184-5

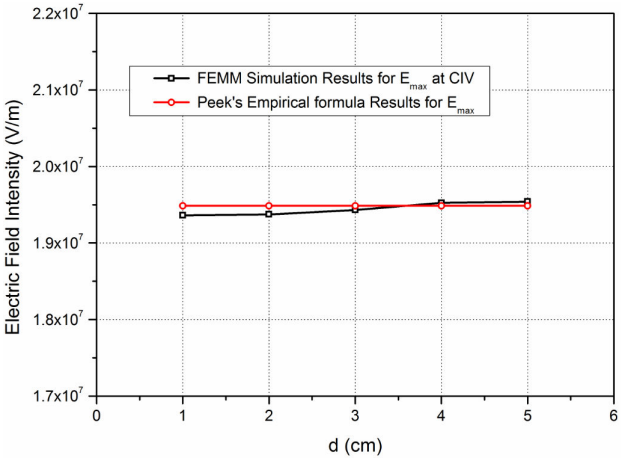

Fig. 11 E_{max} at the *Corona Inception Voltage* with the electrode gap d (*L=500mm, r=30μm and R=15mm*)

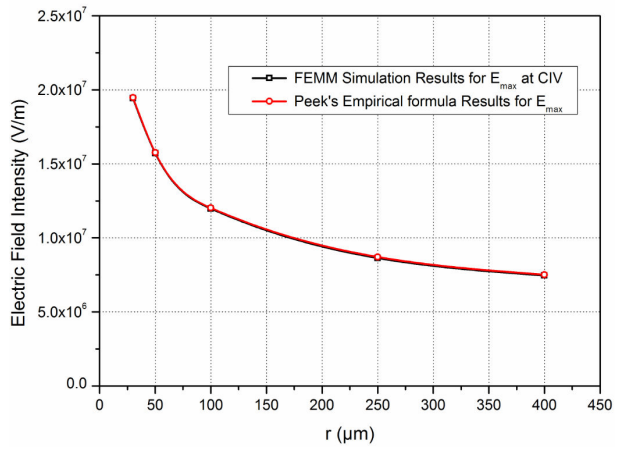

Fig. 12 E_{max} at the *Corona Inception Voltage* with the wire electrode radius r (*L=500mm, d=3cm and R=15mm*)

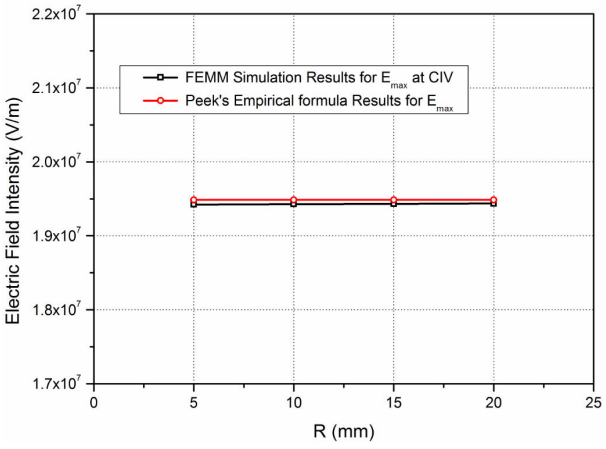

Fig. 13 E_{max} at the *Corona Inception Voltage* with the cylinder radius R (*L=500mm, d=3cm and r=25μm*)

It can be seen in the figures above, that the electric field intensity at the conductor's surface (E_{max} in each case), the exact moment when the corona discharges initiate (*CIV*), depends only on the wire radius r. This comes also in agreement with Peek's empirical formula values according to (9), which coincide with the *FEMM's* simulation results in all cases.

7 Conclusions

A study for the inception voltage of the positive corona discharges (*CIV*) in a typical *wire-cylinder* electrode arrangement in air, under high voltage dc application, has been conducted by implementing the Finite Element Analysis (*FEA*).

Detailed analysis has been carried out in the case of the *wire-cylinder* arrangement, considering different geometrical characteristics of the electrodes such as the electrode gap d and the wire, cylinder electrode radii r and R respectively.

The electric field intensity along the *wire-cylinder* gap axis has been defined, in order to determine the inception voltage in each case and an experimental investigation has been conducted so as to justify the simulation results.

The experimental results were in a good agreement with the simulations data, thus confirming the accuracy of the applied method. Some slight divergences of the investigation results with Peek's empirical formula results (2) may be attributed to the *wire-cylinder* inhomogeneous electric field compared to the parallel wire's geometry.

Simulation and experimental results have shown that the *CIV* was mainly associated to the wire radius r, while the distance d between the electrodes has a secondary importance. On the other hand, the cylinder's radius R seemed to have insignificant affection to the inception of the positive corona discharges.

References:

[1] M. Khalifa, High-Voltage Engineering Theory and Practice, Marcel Dekker inc., New York, 1990.
[2] M.S. Naidu, V. Kamaraju, High Voltage Engineering, Mc Graw Hill, New York, 1996.
[3] C.L. Wadhwa, High Voltage Engineering, New Age International (P) Ltd., 2007.
[4] M. Abdel-Salam, P. Weiss and B. Lieske, Discharges in air from point electrodes in the presence of dielectric plates-experimental results, 27, (1992), pp. 309-319.
[5] K.S.P. Nikas, A.A. Varonos and G.C. Bergeles, Numerical simulation of the flow and the collection mechanisms inside a laboratory scale electrostatic precipitator, J. Electrostatics, 63, (2005), 423-443.

[6] J.H. Kim, H.S. Lee, H.H. Kim and A. Ogata, Electrospray with electrostatic precipitator enhances fine particles collection efficiency, Journal of Electrostatics, 68, (2010), 305-310.
[7] M. Barletta and A. Gisario, Electrostatic spray painting of carbon fibre-reinforced epoxy composites, Progress in Organic Coatings, 64, (2009), 339-349.
[8] A. Jaworek and A.T. Sobczyk, Electrospraying route to nanotechnology: An overview, Journal of Electrostatics, 66, (2008), 197-219.
[9] M. Goldman, Corona discharges and their applications, Physical Science Measurement and Instrumentation, Management and Education - Reviews, IEE Proceedings A, 128, (1981), 298-302.
[10] M. Goldman, A. Goldman and R.S. Sigfmond, The corona discharge, its properties and specific uses, Pure Appl Chem, 57, (1985), 1353-1362.
[11] J.S. Chang, P.A. Lawless and T. Yamamoto, Corona discharge processes, Plasma Science IEEE Transactions, 19, (1991), 1152-1166.
[12] B. Buchet, M. Goldman, A. Goldman, The nature of the permanent current in point to plane corona discharges with direct voltage, Journal of Les Comptes Rendus de l'Académie des sciences, 263, (1966),356-359.
[13] F.W. Peek, Dielectric Phenomena in High Voltage Engineering, McGraw-Hill Press, New York, 1929.
[14] J.J. Lowke and F.D. Alessandro, Onset corona fields and electrical breakdown criteria, J. Appl. Phys., 28, (2003), 2673-2682.
[15] D.B. Phillips, R.G. Olsen and P.D. Pedrow, Corona onset as a design optimization criterion for high voltage hardware, IEEE Trans. Dielectric Electrical Insulation, 7 (6), (2000), 744-751.
[16] V. Amoruso and F. lattarulo, Accurate extension of Peek's law to stranded conductors, European Transactions in Electrical Power, 1, (1), (1991), 15-20.
[17] K. Yamazaki and R.G. Olsen, Application of a corona onset criterion to calculation of corona onset voltage of stranded conductors, IEEE Transactions. Dielectrics and Electrical Insulations, 11, (4), (2004), 674-680.
[18] K.N. Kiousis, A.X. Moronis, Experimental Investigation of EHD Flow in Wire to Cylinder Electrode Configuration, in: 10th IASTED European Conference on Power and Energy Systems, Crete, 2011, pp. 21-26.
[19] K.N. Kiousis and A.X. Moronis, Modeling and Analysis of the Electric Field and Potential Distribution in a Wire-Cylinder Air Gap, Recent Researches in Information Science and Applications, WSEAS International Conference, 2013, pp. 35-40.
[20] K. Kantouna, G.P. Fotis, K.N. Kiousis, L. Ekonomou and G.E. Chatzarakis, Analysis of a Cylinder-Wire-Cylinder Electrode Configuration during Corona Discharge, in: CSCCA, WSEAS, 2012, pp. 204-208.
[21] L. Chen,, J.M.K. MacAlpine, X. Bian, L. Wang and Z. Guan, Comparison of methods for determining corona inception voltages of transmission line conductors, Journal of Electrostatics, 2012, pp. 1-7.
[22] I. Hlavacek and M. Krizek, On a super convergent finite element scheme for elliptic systems. I. Dirichlet boundary condition, Applications of Mathematics, 32, (1987), 131-154.
[23] J.S. Townsend, Electricity in gases, Oxford University press, New York, 1915.

ISBN: 978-1-61804-184-5